DragSail Systems for Satellite Deorbit and Targeted Reentry

Ariel Black[(1)] and David Spencer[(1)]

[(1)] Purdue University, West Lafayette, IN, USA, 47906

ABSTRACT

The safe disposal of spacecraft upon mission completion is necessary to preserve the utility of high-value orbits. Small satellite launches to low Earth orbit and plans for large commercial constellations for global internet service have the potential to exacerbate the orbital debris problem. A dragsail provides an efficient method for accelerating deorbit following the completion of a satellite's operational mission. Unlike propulsive deorbit approaches that require an active host satellite, the passive deorbit approach offered by dragsails does not require a functional host, and dragsails can offer mass savings for deorbit relative to chemical propulsion. Previous dragsail systems have employed flat square sails, which tend to tumble due to atmospheric and solar pressure perturbations. In this paper, a square pyramid geometry for the drag sail is evaluated. The pyramid geometry offers the benefit of passive aerodynamic stability about the maximum drag attitude. Through a six degree-of-freedom simulation, the passive aerodynamic stability provided by the square pyramid geometry is shown, and the deorbit performance of the square pyramid geometry is benchmarked against a typical square sail design. Uncontrolled satellite reentry results in large entry corridor uncertainties, with the range of possible re-entry trajectories often extending over multiple orbits and spanning groundtrack swaths that encompass large portions of the globe. To reduce this uncertainty, dragsails can be applied to achieve targeted reentry capability. The change in ballistic coefficient provided by sail deployment can be used as a control parameter to initiate reentry from a very low orbit, thereby reducing the uncertainty in the reentry corridor and the surface impact footprint. The ability to control the reentry corridor to within a fraction of an orbit reduces the impact of satellite reentry on the air traffic control system and can be used to constrain the probability of debris impact in populated areas. In this work, parametric studies show the efficacy of targeted reentry using dragsail deployment as a control parameter.

1 INTRODUCTION

1.1 Background

As outer space becomes increasingly accessible, the expanding debris in Earth's orbit grows ever more concerning. Historical practice of abandoning defunct spacecraft has resulted in over 8,000 metric tons of detritus and around 20,000 objects larger than 10 cm encircling the Earth, as tracked by the U.S. DoD's Space Surveillance Network (SSN) and illustrated in Fig. 1 [1]. Due to the substantial collision velocities of orbiting bodies (typically 10 km/sec in LEO), even debris as small as 0.2 mm can pose impact risks to Human Space Flight and other critical space assets [2].

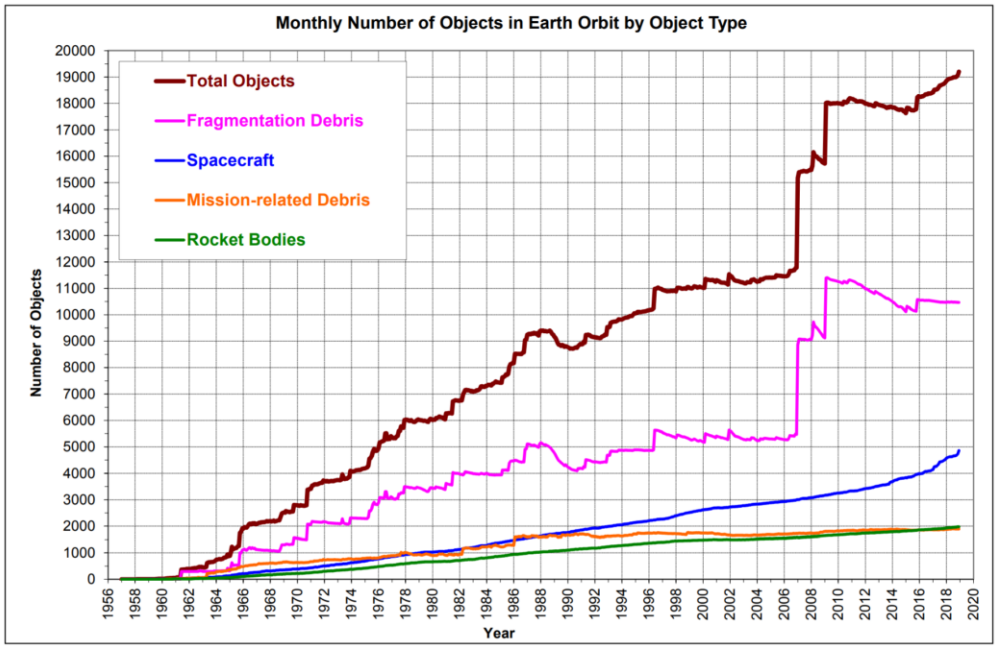

Fig. 1. Objects in Earth orbit by object type; catalogued by the U.S. Space Surveillance Network. "Fragmentation debris" includes satellite breakup debris and anomalous event debris, while "mission-related debris" includes all objects dispensed, separated, or released as part of the planned mission [1].

Controlling the population of orbital debris has become a major priority for the leading space-faring nations of the world, in order to preserve critical orbits and mitigate the risk of catastrophic collisions and the onset of a collisional cascading effect known as Kessler syndrome [3]. The 2018 Nano/Microsat Market Forecast by SpaceWorks estimates that up to 2,600 nanosatellites and microsatellites will be launched into orbit over the next five years [4]. And with the inception of large commercial constellations consisting of hundreds to thousands of small satellites, such as OneWeb and SpaceX Starlink (summarized in Table 1), certain high-value orbits will become congested, placing a priority on end-of-mission deorbit capability.

Table 1. Planned low Earth orbit satellite constellations

Company	Number of Satellites	Satellite Mass (kg)	Constellation Altitudes (km)
Kepler Communications	140	5	500 – 650
LeoSat MA	78	670	1,400
OneWeb	2,956	145	1,000 – 1,200
SpaceX	7,518	386	335 – 346
SpaceX	2,841	386	1,100 – 1,325
SpaceX	1,584	386	550
Spire Global	125	5	450 – 600
Telesat Canada	117	70	1,000
Theia Satellite Network	120	Undisclosed	800

The Inter-Agency Space Debris Coordination Committee (IADC) mandates a maximum orbit lifetime of 25 years post-mission, or 30 years after launch [5]. Space objects will naturally deorbit over the course of their lifetimes; however, at high orbit altitudes, small satellites may not meet the 25-year orbit lifetime requirement without a deorbit device.

Active deorbiting of a host satellite requires attitude control and propulsion capability, and surplus propellant at the end of the mission. Passive deorbit methods, including deployable drag devices, inflatables, and tethers, require no further active control following initiation. The focus of this investigation is the use of dragsails for passive deorbit.

1.2 Overview

To address the growing issue of space debris, the focus of this investigation is the use of dragsails for passive deorbit and targeted re-entry. This paper will discuss:

1. An assessment of the orbit altitude and area/mass ratio combinations that comply with requirements related to deorbit durations and collision probability.
2. Evaluation of the passive aerodynamic stability provided by a square pyramid dragsail geometry, as opposed to the prevalent flat sail design, using an in-house six degree-of-freedom simulation.
3. Studies concerning the efficacy of semi-controlled re-entry using dragsail deployment as a control parameter.

2 ALTITUDE AND AREA/MASS REGIME FOR DEORBIT

2.1 Deorbit Duration Analysis

Deorbit durations for several combinations of area-to-mass ratios at varying initial circular orbit altitudes were determined using the high-fidelity General Mission Analysis Tool (GMAT). The spacecraft ballistic and mass properties in GMAT include drag and solar radiation pressure (SRP) areas and coefficients to inform the orbital dynamics modelling. However, since GMAT only accepts a single constant value for drag coefficient (C_d), rather than varying the C_d with altitude, spacecraft orientation, and atmospheric conditions, an appropriate C_d value must be established. As C_d varies with angle of attack (alpha, α) and side-slip angle (beta, β), and flat dragsails are known to tumble, it is necessary to evaluate the average C_d of a sail over a range of α and β in order to obtain an accurate C_d for GMAT simulations. Direct Simulation Monte Carlo (DSMC) and Free Molecular (FM) Theory simulations reveal that while C_d does not change substantially with altitude variations, it varies significantly with the angle of a spacecraft with respect to the freestream. Table 2 displays C_d dependence on altitude for a flat dragsail with the entire frontal area exposed to the freestream, such that α and β are both 0 deg. Conversely, Fig. 2 illustrates the sensitivity of C_d to changes in α and β. DSMC and FM simulations were performed at a 600 km orbit altitude, increasing the flow angles in 30 deg increments from 0 to 180 deg. The results are based off a 27U CubeSat, 8 m long boom flat sail geometry.

Table 2. Drag coefficient variation with altitude, as determined through DSMC and FM simulations for 0 deg α and β

Altitude (km)	C_d (DSMC)	C_d (FM)
400	2.18	2.19
600	2.32	2.33
800	2.36	2.37

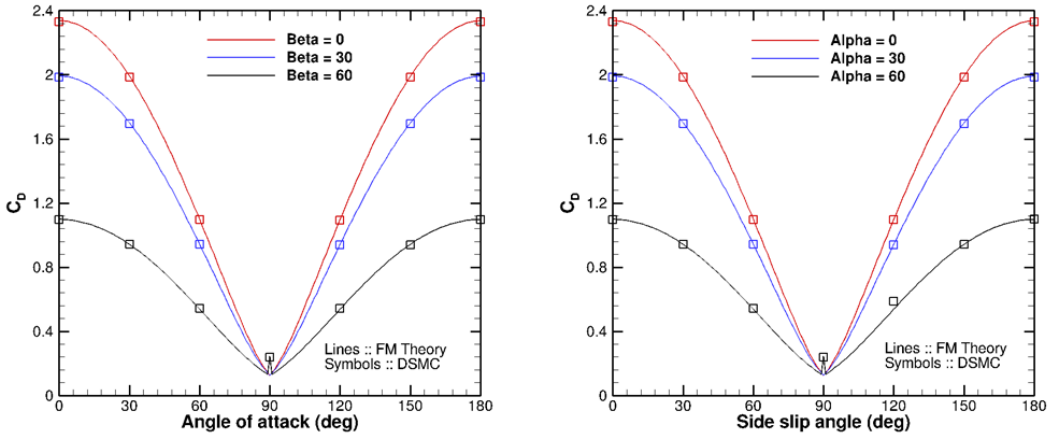

a) b)

Fig. 2. C_d variation at 600 km altitude for a 27U CubeSat, 8 m boom flat sail geometry. a) C_d vs. angle of attack for sideslip angles of 0, 30, and 60 deg. B) C_d vs. sideslip angle for angle of attack of 0, 30, and 60 deg.

The above DSMC analysis resulted in 49 total cases and Cd outputs. These results, plus 751 additional samples obtained through bi-linear interpolation of the DSMC data set, were input into the PRISM Uncertainty Quantification (PUQ) tool [6] to produce a surface response plot of C_d, α and β, as displayed in Fig. 3. Monte Carlo assessment provides an average C_d value of 0.9314, which was used in subsequent GMAT simulations.

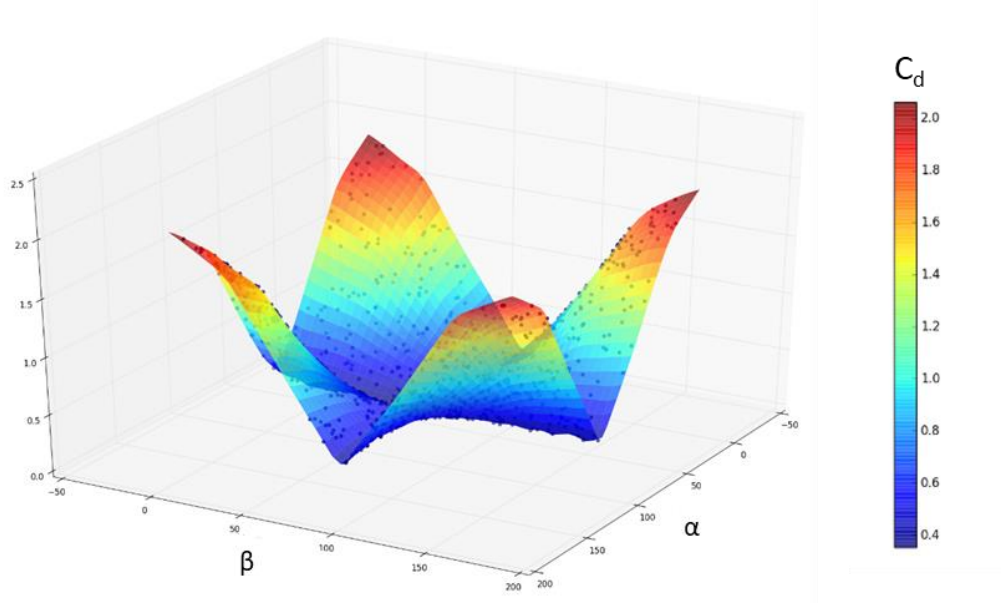

Fig. 3. Direct Simulation Monte Carlo surface response plot of drag coefficient, angle of attach and sideslip angle, generated from 800 samples.

This study investigated seven spacecraft and dragsail combinations, fixing the spacecraft mass and dragsail frontal areas such that discrete area-to-mass ratios of 0.02, 0.15, 0.5, 1, 1.5, 2 and 2.5 were obtained. Each configuration, listed in Table 3, was propagated in GMAT with initial circular orbit altitudes beginning from 400 km and increasing in increments of 50 km until the 25-year restriction was surpassed. The simulation used an SRP area equal to that of the frontal area, a coefficient of reflectivity of 1.8, and a 28.5 deg inclination. The spacecraft was deemed deorbited when it reached an altitude of 110 km.

Table 3. Properties of select spacecraft-dragsail area-to-mass combinations

Spacecraft Mass (kg)	**Frontal Area (m^2)**	**Ballistic Coefficient (kg/m^2)**	**Area-to-Mass (m^2/kg)**
1.33	2	0.71	1.50
12	1.8	7.1577	0.15
24	48	0.5368	2.00
54	135	0.4295	2.50
180	180	1.0736	1.00
400	200	2.1473	0.50
1000	20	53.6826	0.02

GMAT simulations for the above configurations were run using a typical C_d value of 2.2 as well as the average C_d value of 0.9314 obtained from the DSMC evaluation. These simulations confirm that higher area-to-mass ratios yield shorter deorbit durations and enable deorbit from higher altitudes in the regulated timeframe of 25 years, as displayed in Fig. 4. Additionally, the figures show that the choice of C_d has a significant effect on deorbit duration.

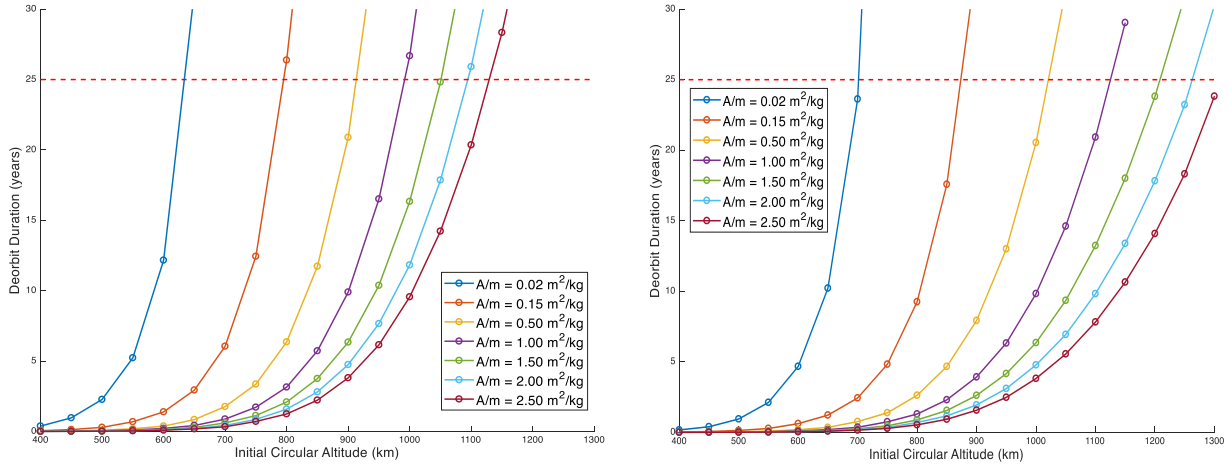

a) b)

Fig. 4: Deorbit duration as a function of initial altitude and area-to-mass ratio. The orbit is inclined 28.5 degrees. a) C_d = 0.9314. b) C_d = 2.2

2.2 Collision Probability Analysis

Probability of collision during the deorbit phase was assessed using NASA's Debris Assessment Software (DAS). Per NASA Technical Standard 8719.14 Appendix B (requirement 4.5-1), the probability of collision with large space objects (>10 cm) must be less than 0.001. Compliance with this requirement is verified using DAS as part of the Federal Communications Commission licensing process. This is a driving requirement for the sizing of dragsail systems; a larger sail area will tend to increase the likelihood of collision during deorbit. While the need to meet a 25-year deorbit timeline results in a minimum required sail area for a given spacecraft mass and initial orbit, the probability of collision requirement may be used to establish a maximum sail area.

Cases were evaluated for a range of host spacecraft configurations, as presented in Table 4. For 1U, 3U, 6U, and 12U CubeSats, a pyramid dragsail with 1 m boom lengths was assumed, resulting in a frontal area of 1.77 m^2. For 27U CubeSats, 180 kg ESPA-class, 400 kg smallsats, and 1000 kg launch vehicle upper stage hosts, a flat dragsail with 3 m booms was assumed, resulting in a frontal area of 18 m^2. In each case, the maximum initial orbit altitude for collision probability compliance was evaluated, along with the maximum altitude that resulted in deorbit within 25 years using DAS. It is seen that for a given spacecraft-dragsail configuration the collision probability requirement the collision probability requirement is generally more restrictive than the 25-year deorbit timeline requirement.

Table 4. Maximum altitude at which probability of collision requirement is met

Host Spacecraft	DragSail Configuration	Sail Geometry	Spacecraft Mass (kg)	DragSail Frontal Area (m^2)	Maximum Deorbit Altitude (km)
1U CubeSat	Spinnaker1	Pyramid	1.33	1.77	1145
3U CubeSat	Spinnaker1	Pyramid	4	1.77	980
6U CubeSat	Spinnaker1	Pyramid	12	1.77	855
12U CubeSat	Spinnaker1	Pyramid	24	1.77	795
27U CubeSat	Spinnaker3	Flat	54	18	845
ESPA-Class SmallSat	Spinnaker3	Flat	180	18	770
SmallSat	Spinnaker3	Flat	400	18	730
LV Upper Stage	Spinnaker3	Flat	1000	18	680

3 PASSIVE AERODYNAMIC STABILITY EVALUATION

Many current dragsail systems employ flat sail designs which tend to tumble due to atmospheric and solar pressure perturbations. Due to the time-varying orientation of the sail relative to the flow direction, the drag achieved from the sail area is not optimal. While flat sails have a larger frontal area than a pyramid sail with the same boom length, a square pyramid geometry, illustrated in Fig. 5, offers the benefit of passive aerodynamic stability about the maximum drag orientation [7-10], as the system center of mass (c.m.) is offset from the center of pressure (c.p.). Since the magnitude of the restoring torque depends upon the c.m.- c.p. distance, a larger offset generates a greater torque for the same applied force.

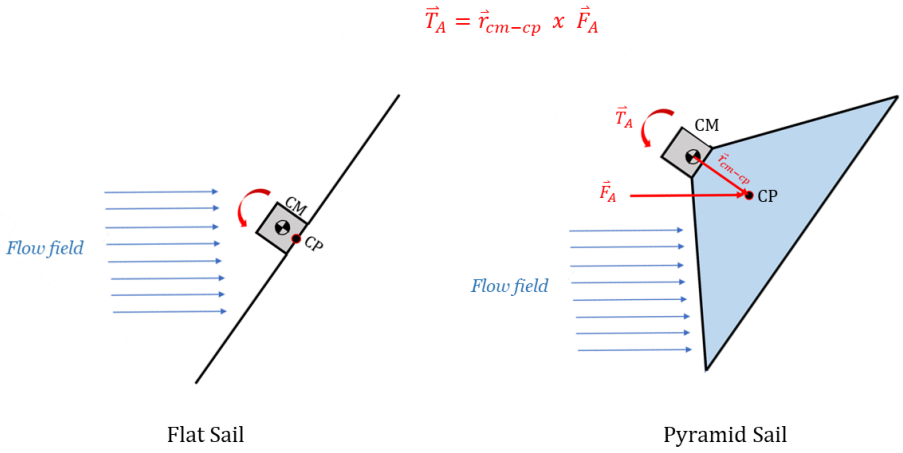

Fig. 5. Flat sail versus square pyramid sail c.m-c.p. offset comparisons

A six degree-of-freedom orbit trajectory and attitude propagator has been developed in the Space Flight Projects Laboratory (SFPL) at Purdue University to evaluate the motion and aerodynamic stability of an arbitrary spacecraft geometry. The model considers the disturbing forces and torques generated from the rarefied aerodynamic environment, gravity gradient perturbations, and solar radiation pressure. We used this propagation tool to perform a comparison between the deorbit and stability of a 1 m boom flat sail and square pyramid sail (with a 70 deg apex half angle) through a free molecular flow regime. Preliminary analysis reveals that in a 28.5 inclination circular orbit, at altitudes of 300 km and lower, both dragsails achieve stability and thus the flat sail deorbits faster due to its larger frontal area. However, at higher altitudes, the flat sail fails to attain stability before deorbiting, as revealed in Fig. 6b, while Fig. 7 shows that the pyramid sail successfully becomes stable and deorbits in less time.

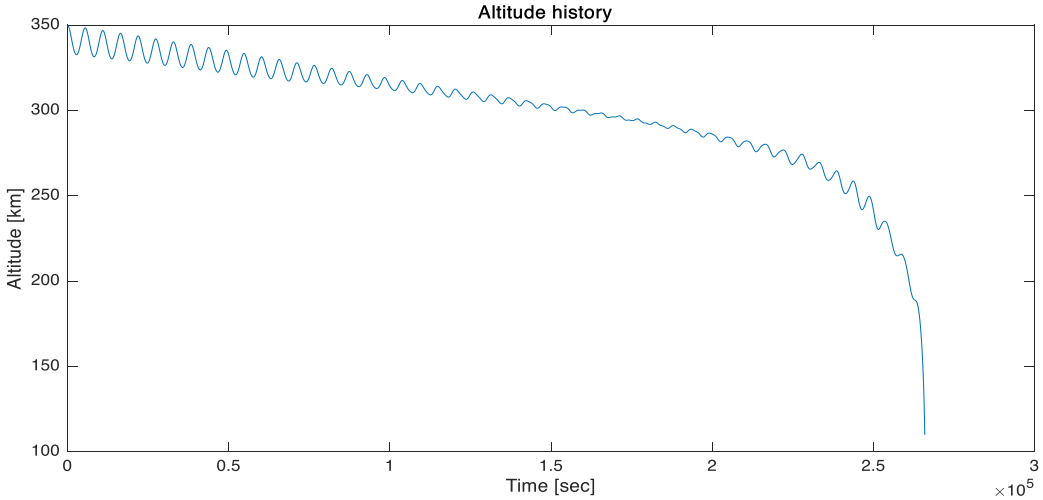

a)

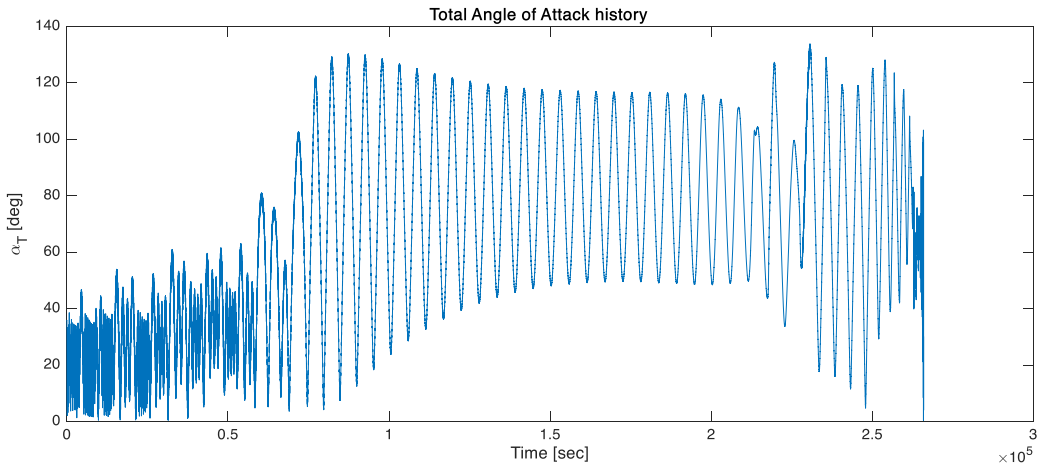

b)

Fig. 6. 1U CubeSat with a 1 m boom flat dragsail deorbit profile. Initial conditions: 350 km orbital altitude, 28.5 deg inclination, 32 deg angle of attack, 20 deg sideslip angle. Deorbit is considered to have occurred at 110 km. a) Altitude history: deorbit occurs in 3.08 days. b) Total angle of attack history. The spacecraft does not trim to a stable orientation.

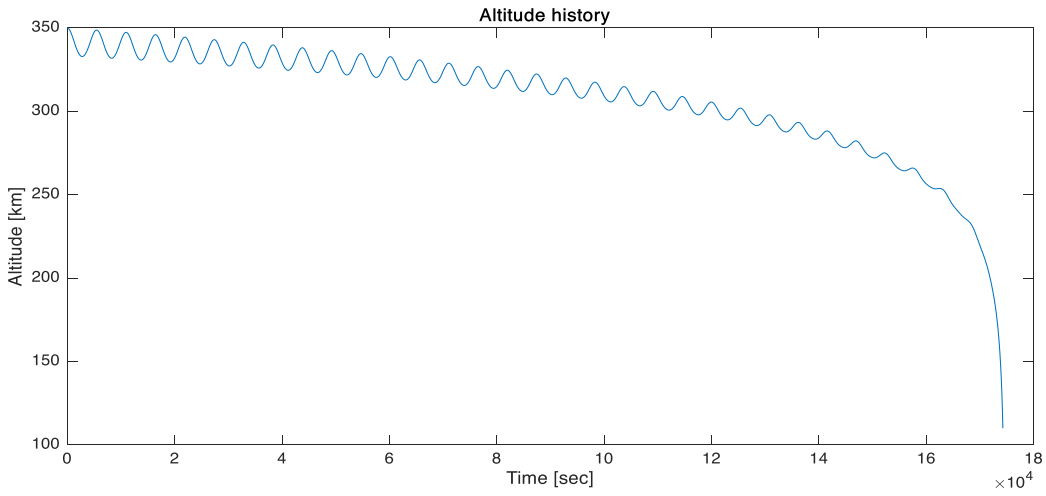

a)

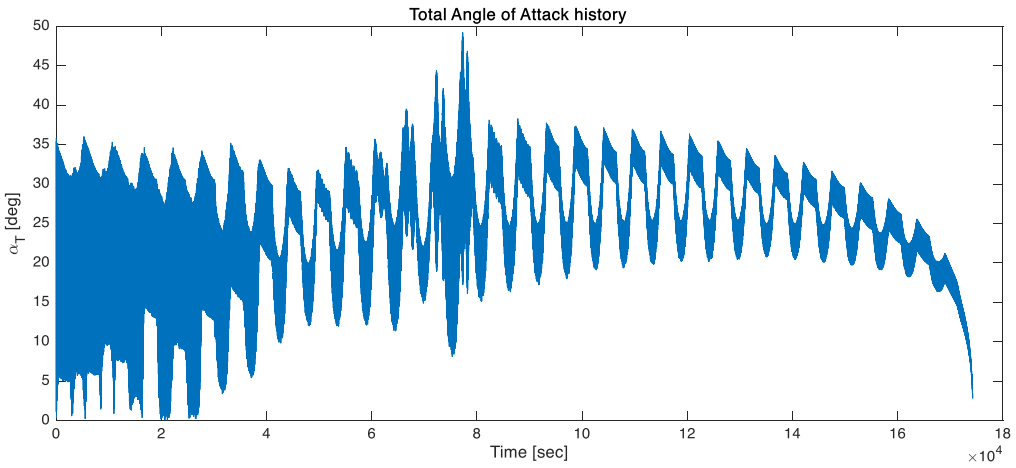

b)

Fig. 7. 1U CubeSat with a 1 m boom pyramid dragsail deorbit profile. Initial conditions: 350 km orbital altitude, 28.5 deg inclination, 32 deg angle of attack, 20 deg sideslip angle. Deorbit is considered to have occurred at 110 km. a) Altitude history: deorbit occurs in 2.02 days. b) Total angle of attack history. The spacecraft trims to a stable orientation.

Future work will involve characterizing the deorbit profile and stability of spacecraft at varying altitudes, inclinations, and angles of attack and sideslip. Additionally, select spacecraft and dragsail geometries will be evaluated.

4 PRELIMINARY ANALYSIS OF TARGETED REENTRY

For Earth orbiting spacecraft that are in the deorbit phase and approaching reentry, dragsail deployment may be used to initiate atmospheric entry and constrain the entry corridor [11]. Uncertainty on the time of reentry often spans multiple orbits, with the consequence that the debris resulting from spacecraft burnup/breakup is not constrained to a specific geographic region. Through deployment of a dragsail at low orbital altitudes, the step increase in drag area provides a drag force that can induce reentry within a fraction of an orbit period, as illustrated in Fig. 8.

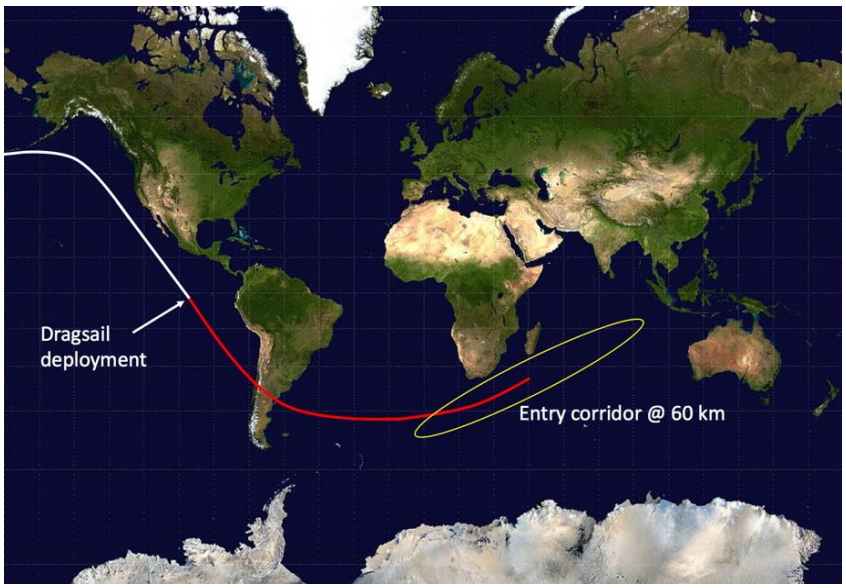

Fig. 8. Dragsail deployment can be used to initiate spacecraft reentry, thereby constraining the entry corridor to a targeted region.

Table 5 shows results for a 6U CubeSat configuration with a spacecraft mass of 12 kg. Without dragsail deployment, from a circular orbit altitude of 160 km the CubeSat will complete approximately five orbits prior to reentry. The uncertainty on the reentry corridor due to atmospheric density variations likely spans multiple orbits and large geographic regions along the orbit groundtrack. If a dragsail with a frontal area of 1.77 m^2 (consistent with the pyramid sail geometry with 1m boom lengths) is deployed at 160 km, the CubeSat will reenter and reach 60 km altitude within a quarter of an orbit. As shown in Table 5, dragsail deployment can occur within the altitude range of up to 260 km and result in reentry within an orbit. The Jacchia 1977 reference atmosphere was used for this analysis. A C_d value of 2.2 is assumed for the host spacecraft prior to dragsail deployment, and a C_d value of 0.93 is assumed following dragsail deployment.

Table 5. For 6U CubeSat host, dragsail deployment in an altitude regime of 100 – 260 km can induce targeted reentry.

		No Sail Deployed (β = 91 kg/m^2)			**Pyramid Sail Deployed (β = 7.3 kg/m^2)**		
Spacecraft Configuration	**Initial Orbit Altitude (km)**	**Area (m^2)**	**Time to Reentry (s)**	**Number of Orbits**	**Area (m^2)**	**Time to Reentry (s)**	**Number of Orbits**
6U CubeSat 12 kg	100	0.06	733	0.14	1.77	348	0.07
	120	0.06	2,331	0.45	1.77	421	0.08
	140	0.06	7,386	1.4	1.77	721	0.14
	160	0.06	26,484	5.0	1.77	1069	0.2
	180	0.06	74,395	14.1	1.77	1495	0.28
	200	0.06	177,530	33.4	1.77	1995	0.38
	220	0.06	365,260	68.5	1.77	2579	0.48
	240	0.06	686,780	128.2	1.77	3363	0.63
	260	0.06	1,229,600	228.5	1.77	4488	0.83
	280	0.06	2,080,200	384.7	1.77	6222	1.15
	300	0.06	3,983,000	625.7	1.77	9066	1.67

Similar results are shown for a 400 kg host spacecraft in Table 6. A flat dragsail with 3m boom lengths is analyzed for this case. Due to the lower area-to-mass ratio of this case relative to the 6U CubeSat, the altitude regime from which sub-orbit reentry can be induced is limited to 150 km or less.

Table 6. For a 400 kg smallsat host, dragsail deployment in an altitude regime of 100 – 150 km can induce targeted reentry.

		No Sail Deployed (β = 534 kg/m^2)			**Pyramid Sail Deployed (β = 24 kg/m^2)**		
Spacecraft Configuration	**Initial Orbit Altitude (km)**	**Area (m^2)**	**Time to Reentry (s)**	**Number of Orbits**	**Area (m^2)**	**Time to Reentry (s)**	**Number of Orbits**
SmallSat 400 kg	100	0.34	1,325	0.25	18	483	0.09
	110	0.34	2,558	0.49	18	867	0.17
	120	0.34	5,232	1.0	18	1447	0.28
	130	0.34	13,617	2.6	18	2249	0.43
	140	0.34	34,421	6.6	18	3347	0.64
	150	0.34	76,201	14.5	18	5091	0.97
	160	0.34	146,890	27.9	18	8259	1.57

Future work will evaluate a broader set of host/dragsail combinations. For selected configurations, a Monte Carlo analysis will be performed with statistical variations on the atmospheric density profile and vehicle drag coefficient to generate distributions on the reentry corridor mapped to an altitude of 60 km.

5 CONCLUSIONS

Deorbit durations for various dragail configurations were established from GMAT simulations for two constant drag coefficients – 0.9314 and 2.2 – to establish the maximum altitude from which the spacecraft can deorbit within the regulated 25-year period. The results reveal that the selection of C_d is crucial for obtaining accurate deorbit performance. Furthermore, collision probability analysis provided the maximum deorbit altitudes for various host spacecraft and dragsail combinations that are in compliance with the 0.001 collision probability restriction.

Initial studies have shown that a square pyramid dragsail geometry with a 70-degree apex half angle provides passive aerodynamic stability at low altitudes, where atmospheric density is sufficient to provide an aerodynamic restoring torque. There is a trade-off between aerodynamic stability and drag area; as the pyramid apex half angle is reduced stability increases (since c.p. moves further aft from the c.m.), while frontal area decreases. Future work will continue to compare flat versus square pyramid sails and evaluate the optimal apex half angle for ideal deorbit conditions.

Finally, preliminary targeted reentry analysis indicates that dragsail deployment may be used to initiate atmospheric entry and constrain the entry corridor. This technique provides the safety benefit of reducing the debris footprint resulting from satellite burnup/breakup.

Acknowledgements

The authors would like to acknowledge the support of our sponsors: NASA and Vestigo Aerospace. We would additionally like to thank Eileen Dukes, Alina Alexeenko, Arun Chinnappan, Anthony Cofer, and Juan Maldonado for their contributions to this work.

REFERENCES

[1] National Aeronautics and Space Administration. "Orbital Debris Quarterly News", The Orbital Debris Program Office, NASA Johnson Space Center, Volume 23, Issues 1&2, May 2019.

[2] Liou, J.C., "Active Debris Removal- A Grand Engineering Challenge for the Twenty-First Century", 21st AAS/AIAA Space Flight Mechanics Meeting. Feb 2011

[3] Kessler, D. J. and Cour-Palais, B. G. (1978): Collision Frequency of Artificial Satellites: The Creation of a Debris Belt, J. of Geophysical Res., Vol. 83, pp. 2637–46.

[4] Spaceworks Enterprises, Inc., "2018 Nano/Microsatellite Market Forecast," 8th Edition, 2018, accessed at http://www.spaceworkscommercial.com/.

[5] National Aeronautics and Space Administration, Process for Limiting Orbital Debris, 2012.

[6] Hunt, M., Haley, B., McLennan, M., Koslowski, M., Murthy, J., and Strachan, A. "PUQ: A code for non-intrusive uncertainty propagation in computer simulations," Computer Physics Communications, Volume 194, pp. 97-107, September 2015.

[7] Long, A.C. and Spencer, D.A., "A Scalable Drag Sail for the Deorbit of Small Satellites," Journal of Small Satellites, Vol. 7, No. 3, December 2018.

[8] Long, A.C. and Spencer, D.A., "A Passively Stable Pyramid Sail for the Deorbit of Small Satellite Constellations," 68th International Astronautical Congress, Adelaide, Australia, September 2017.

[9] Long, A.C. and Spencer, D.A., "Stability of a Deployable Drag Device for Small Satellite Deorbit," AIAA 2016-5676, AIAA SPACE 2016 Conference and Exposition, Long Beach, CA, September 2016.

[10] Long, A., and Spencer, D., "Deployable Drag Device for Launch Vehicle Upper Stage Deorbit," IAC-14-A6.P.82x25843, 65th International Astronautical Congress, Toronto, Canada, September 2014.

[11] Guglielmo, D., Omar, S., Bevilacqua, R., Fineberg, L., Treptow, J., Poffenberger, B. and Johnson, Y., "Drag Deorbit Device: A New Standard Reentry Actuator for CubeSats," Journal of Spacecraft and Rockets, Volume 56, Number 1, January 2019.